

# On the topology of adiabatic passage

L. P. Yatsenko \*, S. Guérin and H. R. Jauslin,  
*Laboratoire de Physique de l'Université de Bourgogne, CNRS,  
BP 47870, 21078 Dijon, France*  
(14 dec 2000)

We examine the topology of eigenenergy surfaces characterizing the population transfer processes based on adiabatic passage. We show that this topology is the essential feature for the analysis of the population transfers and the prediction of its final result. We reinterpret diverse known processes, such as stimulated Raman adiabatic passage (STIRAP), frequency-chirped adiabatic passage and Stark-chirped rapid adiabatic passage (SCRAP). Moreover, using this picture, we display new related possibilities of transfer. In particular, we show that we can selectively control the level which will be populated in STIRAP process in  $\Lambda$  or  $V$  systems by the choice of the peak amplitudes or the pulse sequence.

42.50.Hz, 32.80.Wr, 32.80.Bx

Email: yatsenko@physik.uni-kl.de, guerin@jupiter.u-bourgogne.fr

## I. INTRODUCTION

Adiabatic passage is now a well established tool to achieve complete population transfer between discrete quantum states of atoms and molecules. The main advantage of the processes based on adiabatic passage is their relative robustness with respect to variation of field parameters. The adiabatic passage is achieved with adapted adiabatic variations of at least two *effective* parameters of the total laser field. They can be e.g. the amplitude and the detuning (chirping) or e.g. the amplitudes of two delayed pulses [stimulated Raman adiabatic passage (STIRAP), see [1] for a review]. A chirp can be induced either by direct sweeping of the frequency of one laser pulse [2–8], or as proposed very recently by a Stark shift of the transition due to an additional laser field [process named Stark chirped rapid adiabatic passage (SCRAP)] [9,10]. The use of adiabatic passage for multiple photon absorption and emission processes accompanying momentum exchanges between the atom and the laser fields have also been recently investigated [11–13].

In this paper, we show that all of these adiabatic passage processes can be understood by an analysis of the topology of the surfaces of eigenenergies as functions of the field parameters. This tool allows us to derive new ways of controlling population transfer, related to STIRAP.

The tools of analysis follow Ref. [13]. From an effective Hamiltonian, which can be constructed by quasi-resonant approximations combined with adiabatic eliminations from the complete Hamiltonian of the considered process, we determine and analyze the topology of the energy surfaces, which display conical intersections and avoided crossings due to resonances. In the general cases, these resonances are induced by the fields (dynamical resonances) [13,14]. The adiabatic dynamics of the process is determined by the topology of these energy surfaces and can be completely predicted. The dynamics governed by the time-dependent Schrödinger equation is thus reduced to the topology of the solutions of the time-independent Schrödinger equation.

## II. TOPOLOGY OF CHIRPING

The essence of the adiabatic passage induced by chirping is captured with the effective two-state Hamiltonian in the rotating wave approximation [4,15]

$$H(t) = \frac{\hbar}{2} \begin{bmatrix} 0 & \Omega(t) \\ \Omega(t) & 2\Delta(t) \end{bmatrix}, \quad (1)$$

---

\*Permanent address: Institute of Physics, National Academy of Sciences of Ukraine, prospekt Nauky, 46, Kiev-22, 03650, Ukraine

which describes the radiative interaction between a two-level system (states  $|1\rangle$  and  $|2\rangle$ ) and the quasi-resonant laser field through the effective Rabi frequency  $\Omega(t)$  and the effective detuning  $\Delta(t)$ . We have assumed that spontaneous emissions are negligibly small on the time scale of the pulse duration. The population resides initially in the state  $|1\rangle$ .

In these processes,  $\Omega(t)$  stands for a one- or multi-photon Rabi frequency (depending on the process studied, see e.g. Ref. [8] for an effective two-photon chirping) and

$$\Delta(t) = \Delta_0(t) + S(t) \quad (2)$$

is the sum of the detuning from the one- or multi-photon resonance and of the effective dynamical Stark shift. This effective dynamical Stark shift  $S(t)$  results from the difference of the dynamical Stark shifts associated to the two energy levels and produced by the laser fields non resonant with the other levels of the system. For the *direct chirping*, the detuning from the resonance  $\Delta_0(t)$  is time dependent due to an active sweeping of the laser frequency. The dynamical Stark shifts  $S(t)$  are in general detrimental since they shift the levels away from the resonance. For the *Stark chirping*, the quasi-resonant laser frequency is not chirped (the detuning  $\Delta_0$  is time independent); the time dependence of the effective detuning  $\Delta(t) = \Delta_0 + S(t)$  is only due to Stark shifts which are induced by the laser pulses [9,10].

The process can be completely described by the diagram of the two surfaces

$$\lambda_{\pm}(\Omega, \Delta) = \frac{\hbar}{2} \left( \Delta \pm \sqrt{\Omega^2 + \Delta^2} \right) \quad (3)$$

which represent the eigenenergies as functions of the instantaneous effective Rabi frequency  $\Omega$  and detuning  $\Delta$  (see Fig. 1). All the quantities are normalized with respect to a characteristic detuning denoted  $\Delta_{\text{in}}$ . They display a conical intersection for  $\Omega = 0, \Delta = 0$  induced by the crossing of the lines characterizing the states  $|1\rangle$  and  $|2\rangle$  for  $\Omega = 0$  and various  $\Delta$ . The way of passing around or through this conical intersection is the key of the successful transfer. Three generic curves representing all the possible passages with a negative initial detuning  $-|\Delta_{\text{in}}|$  are shown. Note that the three other equivalent curves with a positive initial detuning have not been drawn. The path (a) corresponds to a direct chirping of the laser frequency from the initial detuning  $-|\Delta_{\text{in}}|$  to the final one  $+|\Delta_{\text{in}}|$ . The paths (b) and (c) correspond to SCRAP with  $\Delta_0 = -|\Delta_{\text{in}}|$ . For the path (b), while the quasi-resonant pump pulse is off, another laser pulse (the Stark pulse, which is far from any resonance in the system) is switched on and induces positive Stark shifts  $S(t) > 0$  (the Stark pulse frequency is chosen with this aim). The Stark pulse makes thus the eigenstates get closer and induces a resonance with the pump frequency. This resonance is mute since the pump pulse is still off, which results in the true crossing in the diagram. The pump pulse is switched on after the crossing. Later the Stark pulse decreases while the pump pulse is still on. Finally the pump pulse is switched off. As shown in the diagram, the adiabatic following of the path (b) induces the complete population transfer from state  $|1\rangle$  to state  $|2\rangle$ . The path (c) leads exactly to the same effect: The pump pulse is switched on first (making the eigenstates repel each other as shown in the diagram) before the Stark pulse  $S(t) > 0$  which is switched off after the pump pulse.

The conditions for adiabatic passage involving one unique statevector are standard: adiabatic evolution is satisfied when the rate of changes  $|\dot{\Theta}(t)|$  in the mixing angle  $\Theta(t)$ , defined as  $\tan 2\Theta(t) = \Omega(t)/\Delta(t)$ ,  $-\pi \leq 2\Theta(t) \leq 0$ , is much smaller than the separation of the eigenvalues  $|\lambda_+(t) - \lambda_-(t)|/\hbar = \sqrt{\Omega^2(t) + \Delta^2(t)}$ :

$$|\dot{\Theta}(t)| \ll \sqrt{\Omega^2(t) + \Delta^2(t)}. \quad (4)$$

The peak amplitudes, the delay between the two fields and the pulse shapes are chosen such that these conditions of adiabatic passage are met. Detailed conditions of adiabatic passage can be found in [10] for delayed Gaussian pulses.

### III. TOPOLOGY OF STIMULATED RAMAN ADIABATIC PASSAGE

The adiabatic passage induced by two delayed laser pulses, the well known process of STIRAP, produces population transfer in  $\Lambda$  systems (see Fig. 2a). (The pump field couples the transition 1-2 and the Stokes field couples the transition 2-3.) It is known that, the initial population being in state  $|1\rangle$ , the complete population transfer is achieved with delayed pulses, either (i) with a so-called counterintuitive temporal sequence (Stokes before pump) for various detunings as identified in Refs [16,17], or (ii) with a two-photon resonant (or quasi-resonant) pulses but far from the one-photon resonance with the intermediate state  $|2\rangle$ , for any pulse sequence (demonstrated in the approximation of adiabatic elimination of the intermediate state [18]). Here we revisit the STIRAP process through the topology of the associated surfaces of eigenenergies as functions of the two field amplitudes.

Our results are also valid for ladder and  $V$  systems.

We also show the following results which are new to our knowledge: (i) we can transfer the population to state  $|3\rangle$  with intuitive (as with counterintuitive) specific quasi-resonant pulses *without invoking the approximation of adiabatic elimination*, (ii) with specific quasi-resonant pulses, we can *selectively* transfer the population to state  $|2\rangle$  for an *intuitive* sequence or to state  $|3\rangle$  for a *counterintuitive* sequence, and (iii) with an intuitive or counterintuitive sequence, we can *selectively* transfer the population to state  $|2\rangle$  or to state  $|3\rangle$  playing on the *detunings* and on the *peak pulse amplitudes ratio*. We remark that the selectivity (ii) has been demonstrated in the case of exact two-photon resonant pulses [19]. This last result is however not robust since it depends on using precisely determined total pulse areas.

We also analyze the counterpart of the previous processes in  $V$  systems (see Fig. 2b): the initial population being in state  $|2\rangle$ , we show that with specific non-resonant pulses, (i) we can *selectively* transfer the population to state  $|1\rangle$  for an intuitive sequence or to state  $|3\rangle$  for a counterintuitive sequence; (ii) we can *selectively* transfer the population to state  $|1\rangle$  or to state  $|3\rangle$  playing on the ratio of the peak pulse amplitudes.

The most general Hamiltonian in the rotating wave approximation for these processes reads

$$\mathbf{H}(t) = \frac{\hbar}{2} \begin{bmatrix} 0 & \Omega_P(t) & 0 \\ \Omega_P(t) & 2\Delta_P & \Omega_S(t) \\ 0 & \Omega_S(t) & 2(\Delta_P - \Delta_S) \end{bmatrix}, \quad (5)$$

with  $\Omega_j(t)$ ,  $j = P, S$  the one photon Rabi frequencies associated respectively to the pump pulse (of carrier frequency  $\omega_P$ ) and the Stokes pulse (of carrier frequency  $\omega_S$ ). We have assumed that the states  $|1\rangle$  and  $|3\rangle$  have no dipole coupling and that spontaneous emission from the upper state  $|2\rangle$  is negligibly small on the time scale of the pulse duration. The rotating wave transformation is valid if  $\Omega_P(t) \ll |E_2 - E_1|$  and  $\Omega_S(t) \ll |E_3 - E_2|$ , where  $E_j$ ,  $j = 1, 2, 3$  are the energies associated to the bare states  $|j\rangle$

The detunings  $\Delta_P$  and  $\Delta_S$  are one-photon detunings with respect to the pump and Stokes frequencies respectively and

$$\delta = \Delta_P - \Delta_S \quad (6)$$

is the two-photon detuning.

For  $\Lambda$ , ladder and  $V$  systems (see respectively Fig. 2a, b and c), the one-photon detunings  $\Delta_P$ ,  $\Delta_S$  are respectively defined as

$$\hbar\Delta_P = E_2 - E_1 - \hbar\omega_P, \quad \hbar\Delta_S = E_2 - E_3 - \hbar\omega_S, \quad (7a)$$

$$\hbar\Delta_P = E_2 - E_1 - \hbar\omega_P, \quad \hbar\Delta_S = E_2 - E_3 + \hbar\omega_S, \quad (7b)$$

$$\hbar\Delta_P = E_2 - E_1 + \hbar\omega_P, \quad \hbar\Delta_S = E_2 - E_3 + \hbar\omega_S. \quad (7c)$$

In what follows we study the topology of the eigenenergy surfaces for various generic sets of the parameters. The topology depends on the detunings which determine the relative position of the energies at the origin. We study various *quasi-resonant* pulses in the sense that the detunings are small with respect to the associated peak Rabi frequencies, i.e.

$$\Delta_P \lesssim \max_t(\Omega_P), \quad \Delta_S \lesssim \max_t(\Omega_S), \quad (8a)$$

$$\delta \lesssim \max_t(\Omega_P), \quad \delta \lesssim \max_t(\Omega_S). \quad (8b)$$

Allowing large enough amplitudes imply three generic cases for  $\delta > 0$ , which are referred to 213, 132 and 123 (these number sets are associated to the eigenenergies for zero field amplitudes from the smallest to the biggest). Three other symmetric and thus equivalent cases (referred as 312 symmetric with 213, 231 with 132 and 321 with 123) appear for  $\delta < 0$ .

### A. The cases 213 and 132

The case 213 corresponds to  $\Delta_S < \Delta_P < 0$  and its symmetric 312 to  $0 < \Delta_P < \Delta_S$ . One example for the case 213 is diagrammed in Fig. 3 for  $\Delta_P = -\delta/2$  and  $\Delta_S = -3\delta/2$ .

The case 132 corresponds to  $0 < \Delta_S < \Delta_P$  (and its symmetric 231 to  $\Delta_P < \Delta_S < 0$ ) as diagrammed in Fig. 4 for  $\Delta_P = 3\delta/2$  and  $\Delta_S = \delta/2$ . Fig. 4 shows that the topology of the 132 case is similar to the topology of the 213 case.

In both cases, the surface continuously connected to the state  $|2\rangle$  is isolated from the two other surfaces which present a conical intersection for  $\Omega_S = 0$  (resp.  $\Omega_P = 0$ ) in the 213 configuration (resp. 132 configuration). This crossing corresponds to a mute resonance as described above for chirping. The topologies shown on the respective figures 3 and 4 are generic for the condition

$$\Delta_P \Delta_S > 0, \quad (9)$$

with respectively

$$|\Delta_P| < |\Delta_S| \quad \text{and} \quad |\Delta_P| > |\Delta_S|. \quad (10)$$

In the following, we describe in detail the 213 case (see Fig. 3). For the process in  $\Lambda$  or ladder systems, where the initial population resides in state  $|1\rangle$ , two different adiabatic paths lead to the complete population transfer, depending on the pulse sequence. The path denoted (a) corresponds to an intuitive sequence for the increasing pulses. The pump pulse is switched on first, making the levels connected to the states  $|1\rangle$  and  $|2\rangle$  repel each other (dynamical Stark shift) until the level connected to  $|1\rangle$  crosses the level connected to  $|3\rangle$ . The Stokes pulse is switched on after the crossing. Next the two pulses can decrease in any sequence. The path (b) is associated to a counterintuitive sequence for the decreasing pulses. The two pulses can be switched on for any sequence. The pump pulse has to decrease through the crossing when the Stokes pulse is already off. These two results are valid even without application of adiabatic elimination. The conditions of adiabaticity are very similar to the ones of the chirping case (4).

The  $V$  systems are uninteresting in these cases since the final population comes back to the state  $|2\rangle$  for any pulse sequence.

### B. The case 123

The case 123 corresponds to  $\Delta_S < 0 < \Delta_P$  and its symmetric 321 to  $\Delta_P < 0 < \Delta_S$ . One example for the case 123 is diagrammed in Figs 5 for  $\Delta_P = \delta/2$  and  $\Delta_S = -\delta/2$ . The topology shown on this figure is generic for the condition

$$\Delta_P \Delta_S < 0. \quad (11)$$

In this configuration, two conical intersections involve the intermediate surface, one with the lower surface and another with the upper surface. This topology gives here more possibilities for transfer: *the combined choice of the pulse sequence and the ratio of the peak amplitudes allows the selective transfer into the two other states.*

Figure 5 shows that, for the process in  $\Lambda$  (or ladder) systems, two different adiabatic paths lead to different complete population transfers, depending on the pulse sequence. The path (a) characterizes an intuitive pulse sequence (for decreasing pulses) and allows to populate at the end the state  $|2\rangle$ . The Stokes and pump pulses are switched on in any sequence and the pump pulse is switched off before the Stokes. The paths (b) characterizes a counterintuitive pulse sequence (for increasing pulses) and allows to populate at the end the state  $|3\rangle$ . The Stokes pulse is switched on before the pump and the pulses are switched off in any sequence. We can thus selectively populate the states  $|2\rangle$  or  $|3\rangle$  provided the peak amplitudes are sufficiently strong to induce the adiabatic path to cross the intersection involved.

For the process in  $V$  systems, the paths (a) and (c) of Fig. 5 show the respective selective transfer into the states  $|1\rangle$  or  $|3\rangle$ .

Figure 6 corresponds to the same topology of Fig. 5 but with a different path (a). Figure 6 shows that, for  $\Lambda$  (or ladder) systems with counterintuitive sequences, we can selectively populate the states  $|2\rangle$  or  $|3\rangle$  if the pulse sequence are designed differently in their sequence and their peak amplitude. The paths (b) corresponds to the previous path (b) of Fig. 5 and allows to populate at the end the state  $|3\rangle$ . The path (a) is characterized by a pump pulse (still switched on after the Stokes pulse) longer and of smaller peak amplitude and allows to populate at the end the state  $|2\rangle$ . Note that we can obtain a similar path (a) with a counterintuitive pulse sequence and equal peak amplitudes if the detuning  $\Delta_P$  is taken smaller so that the crossing for  $\Omega_S = 0$  is pushed to higher pump pulse amplitude  $\Omega_P$ .

For  $V$  systems, Fig. 6 shows that this selectivity [paths (a) and (c)] also occurs (for any sequence of the pulse).

## IV. DISCUSSION AND CONCLUSIONS

In this article we have applied simple geometrical tools to two- and three-level systems in the rotating wave approximation to classify all the possibilities of complete population transfer by adiabatic passage, when the two-level system is driven by a chirped laser pulse and the three-level system by two delayed pulses. We have shown that

the complete transfer by adiabatic passage is intrinsically related to the topology of the eigenenergy surfaces. We have found the following new results in the three-level systems such as, in  $\Lambda$  or ladder systems, (i) robust population transfer to the state  $|3\rangle$  by an intuitive sequence of quasi-resonant pulses, (ii) robust selective transfer to the states  $|2\rangle$  and  $|3\rangle$  depending on the design of the pulses (lengths, amplitudes and delay).

The topology gives information on the dynamics for purely adiabatic passage. For real pulses of finite duration one has to complement these information with the analysis of the effects of non-adiabatic corrections. Figure 7 shows numerical calculations that illustrate some of the predictions of the analysis of section III. It displays the populations of the states  $|2\rangle$  and  $|3\rangle$  at the end of the pulses for intuitive and counterintuitive sequences with a large pulse area. The boundaries of the areas of efficient transfer (black areas) are predicted quite accurately by the topology analysis: They are determined by (i) the straight lines (thick full lines)  $\Delta_P = 0$  and  $\Delta_S = 0$  coming from the inequalities (9) and (11) and (ii) the branches of the hyperbolas (dashed lines)

$$\Delta_S = \Delta_P - \frac{(\Omega_{\max})^2}{4\Delta_P}, \quad (12)$$

$$\Delta_P = \Delta_S - \frac{(\Omega_{\max})^2}{4\Delta_S}, \quad (13)$$

which are determined from the positions of the conical intersections. Figure 7 shows that the efficiency of the robust population transfer to the states  $|2\rangle$  or  $|3\rangle$  is identical for the intuitive and counterintuitive sequences except in two regions: (i) areas bounded by  $\Delta_P\Delta_S < 0$  and the branches of the hyperbolas, where the population is transferred in a robust way to state  $|2\rangle$  for the intuitive sequence or to state  $|3\rangle$  for the counterintuitive sequence and (ii) a area (smaller for longer pulse areas) near the origin where non adiabatic effects are strong for the intuitive sequence and where the population transfer depends precisely on the pulse areas for this intuitive sequence (see the comments below). Non adiabatic effects, which are smaller for larger pulse areas, also occur near the boundary regions.

For the concrete realization with finite pulses of moderate areas, we have to analyze the precise influence of non adiabatic effects. In the following we study these non adiabatic effects referring to Fig. 3 supposing that the detunings are small enough with respect to the speed of the process to yield non adiabatic transitions.

In the intuitive case, at the beginning of the process, the states  $|1\rangle$  and  $|2\rangle$  are coupled by the pump pulse, and thus non adiabatic transitions can occur near the origin between the surfaces connected to  $|1\rangle$  and  $|2\rangle$ . In the counterintuitive case, at the beginning of the process, state  $|1\rangle$  is not coupled to the other levels and there are no non adiabatic transitions near the origin. At the end of the process, the adiabatic path ending in  $|3\rangle$  is not coupled to the other levels, implying again absence of non adiabatic transitions near the origin. We thus recover the well known fact that resonant STIRAP is more favorable with counterintuitive pulse sequence and leads to Rabi oscillations in the intuitive case.

The consequences of the topology on the population transfer with exact resonances at  $\Omega_S = 0$ ,  $\Omega_P = 0$  giving rise to degeneracies will be discussed in a forthcoming work.

## V. ACKNOWLEDGMENTS

We acknowledge support by INTAS 99-00019. LY thanks l'Université de Bourgogne for the invitation during which this work was accomplished. We thank K. Bergmann and R. G. Unanyan for useful discussions.

Figure 1

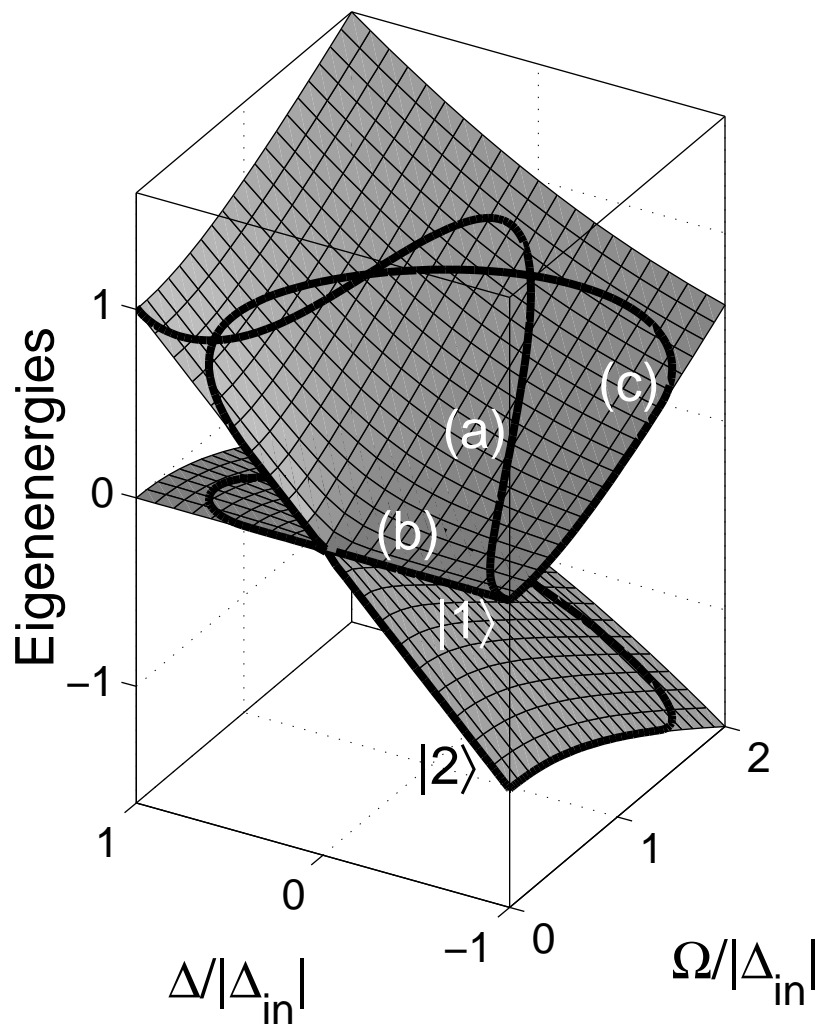


FIG. 1. Surfaces of eigenenergies (in units of  $|\Delta_{in}|$ ) as functions of  $\Omega/|\Delta_{in}|$  and  $\Delta/|\Delta_{in}|$ . Three different paths, denoted (a), (b) and (c) are depicted: (a) corresponds to a direct chirping and (b) and (c) to SCRAP.

Figure 2

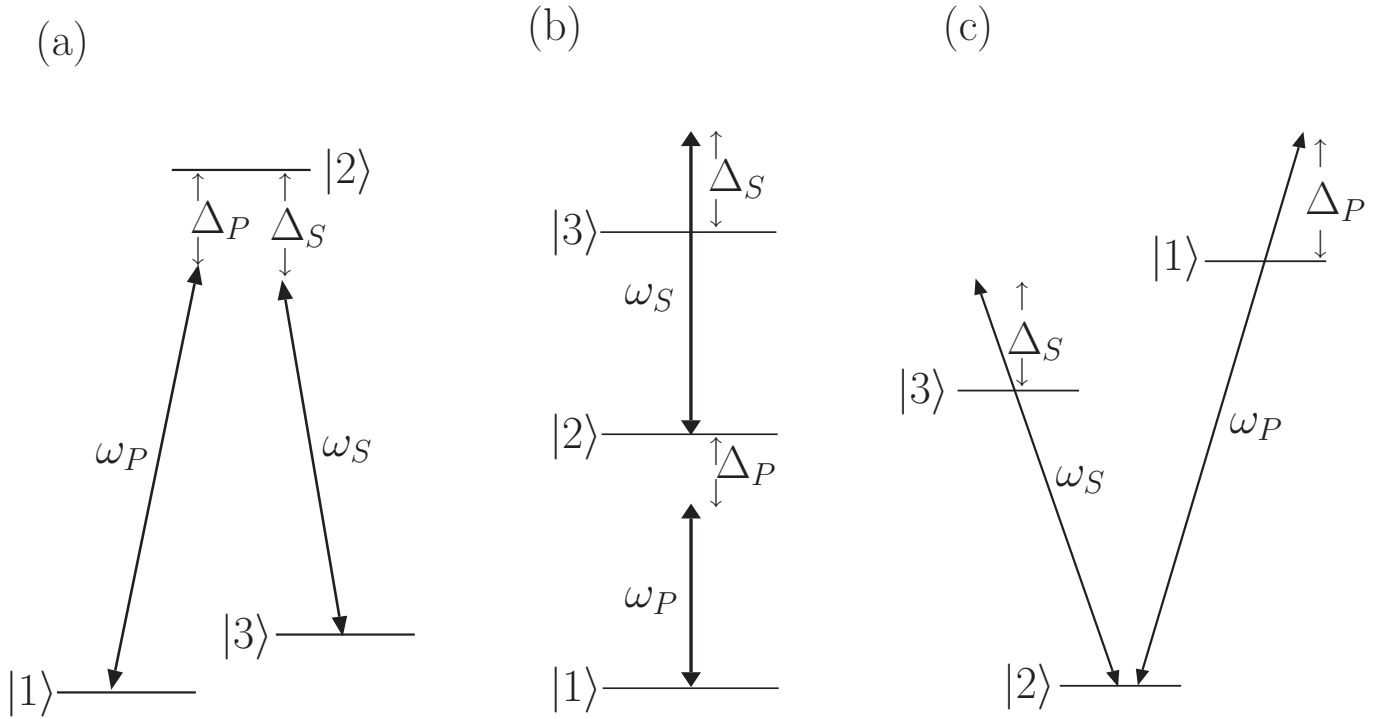


FIG. 2. Diagram of linkage patterns between three atomic states showing pump ( $P$ ) and Stokes ( $S$ ) transitions and the various detunings for (a)  $\Lambda$  and (b)  $V$  systems.

Figure 3

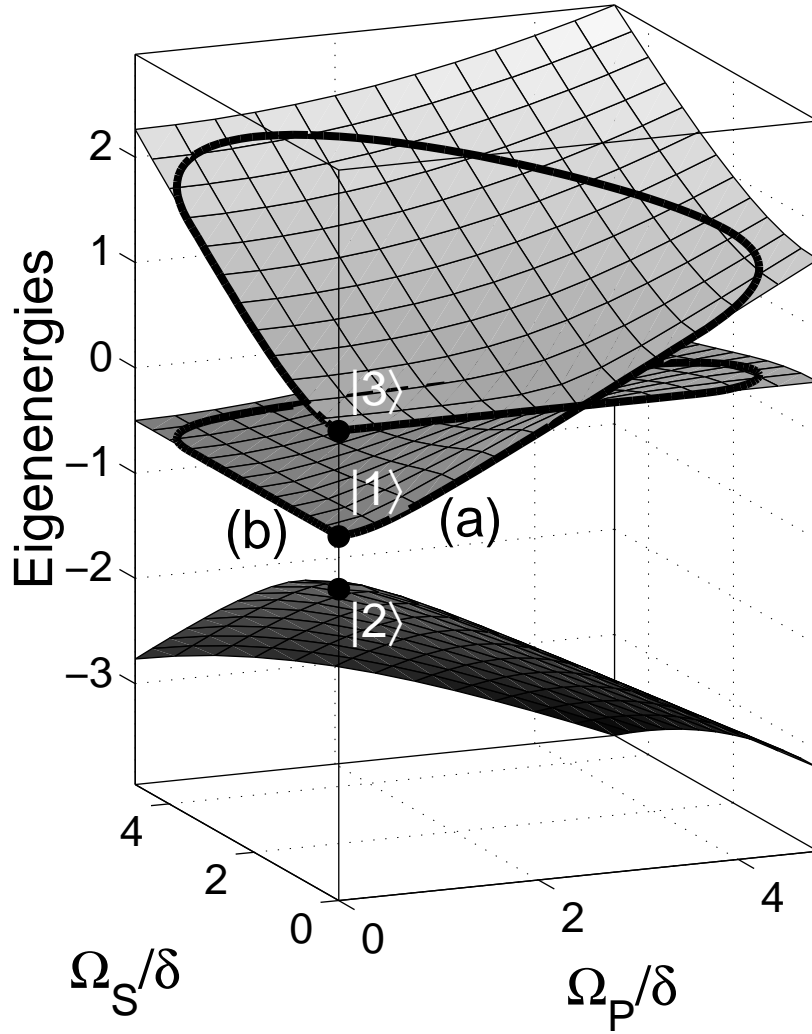


FIG. 3. Surfaces of eigenenergies (in units of  $\delta$ ) as functions of  $\Omega_P/\delta$  and  $\Omega_S/\delta$  for the case 213. The paths (a) and (b) (constructed with delayed pulses of the same length and peak amplitude) correspond respectively to the intuitive and counterintuitive pulse sequences in  $\Lambda$  or ladder systems (for which the initial population resides in state  $|1\rangle$ ).

Figure 4

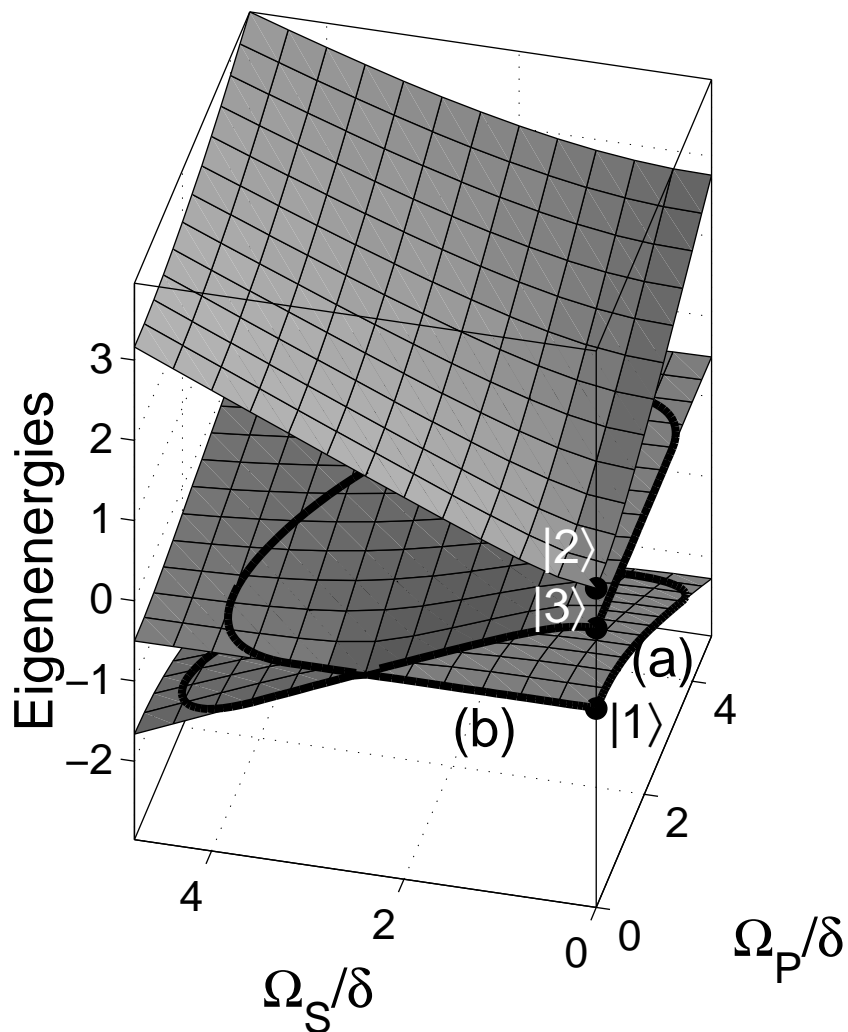


FIG. 4. Surfaces of eigenenergies (in units of  $\delta$ ) as functions of  $\Omega_P/\delta$  and  $\Omega_S/\delta$  for the case 132. The paths (a) and (b) (with pulses of the same length and peak amplitude) correspond respectively to the intuitive and counterintuitive pulse sequences in  $\Lambda$  or ladder systems.

Figure 5

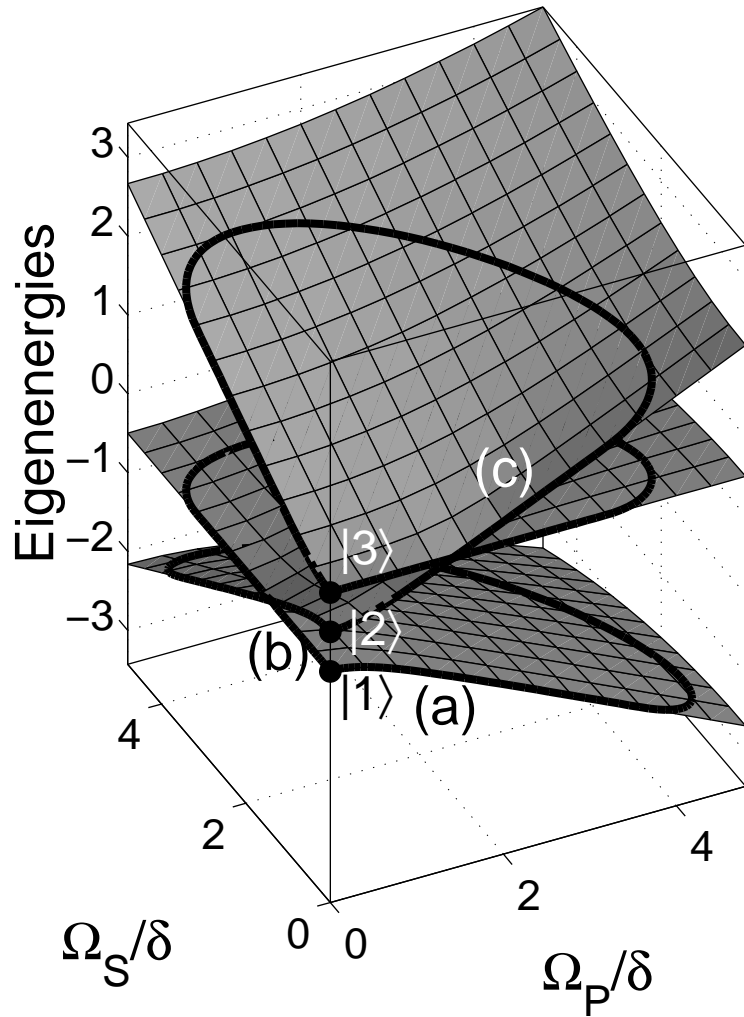


FIG. 5. Surfaces of eigenenergies (in units of  $\delta$ ) as functions of  $\Omega_P/\delta$  and  $\Omega_S/\delta$  for the case 123. The paths (a) and (b) (with pulses of the same length and peak amplitude) correspond respectively to the intuitive (transfer to  $|2\rangle$ ) and counterintuitive (transfer to  $|3\rangle$ ) pulse sequences in  $\Lambda$  or ladder systems leading to the selective transfer. The paths (a) and (c) correspond to the selective transfer in  $V$  systems (for which the initial population resides in  $|2\rangle$ ), respectively to  $|1\rangle$  and  $|3\rangle$ .

Figure 6

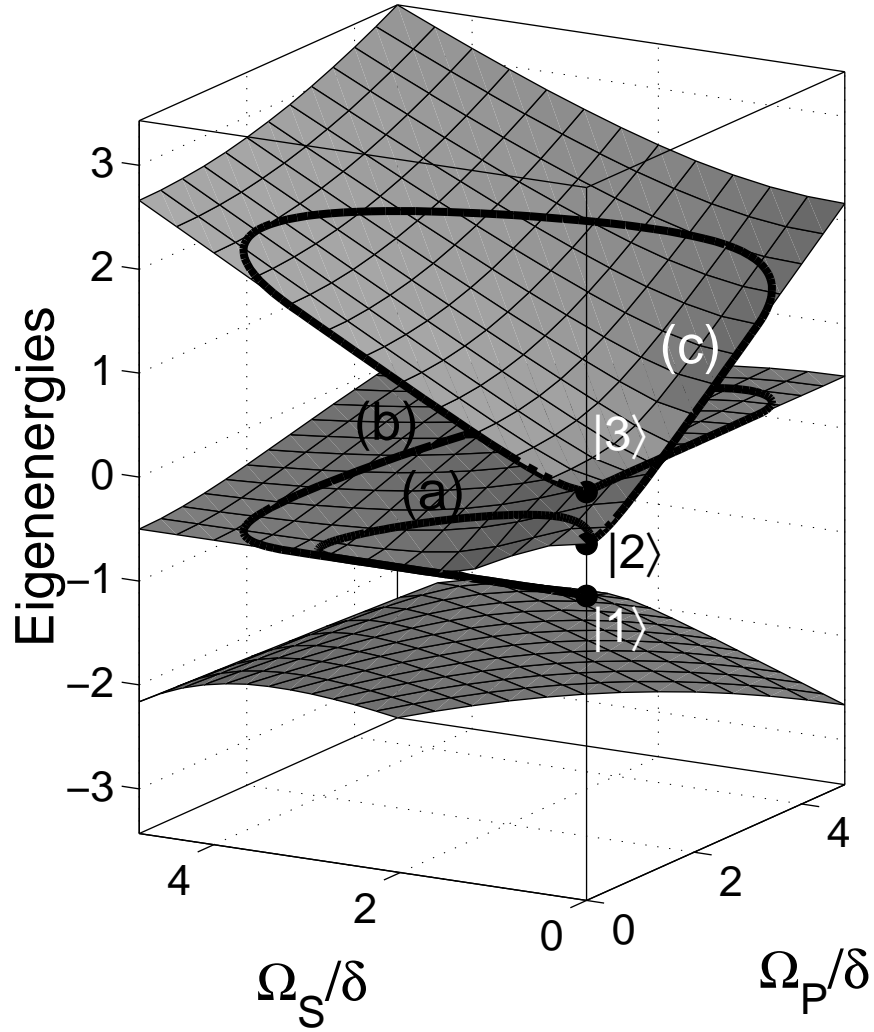


FIG. 6. Surfaces of eigenenergies with the same parameters as Fig. 5 showing the selective transfer with pulses of different peak amplitudes and length. For counterintuitive sequences in  $\Lambda$  or ladder systems, the path (b) [corresponding to the path (b) of Fig. 5] shows the transfer to  $|3\rangle$ , and the path (a) (with pulses of different length and peak amplitude) characterizes the transfer to  $|2\rangle$ . The paths (a) and (c) correspond to the selective transfer in  $V$  systems.

Figure 7

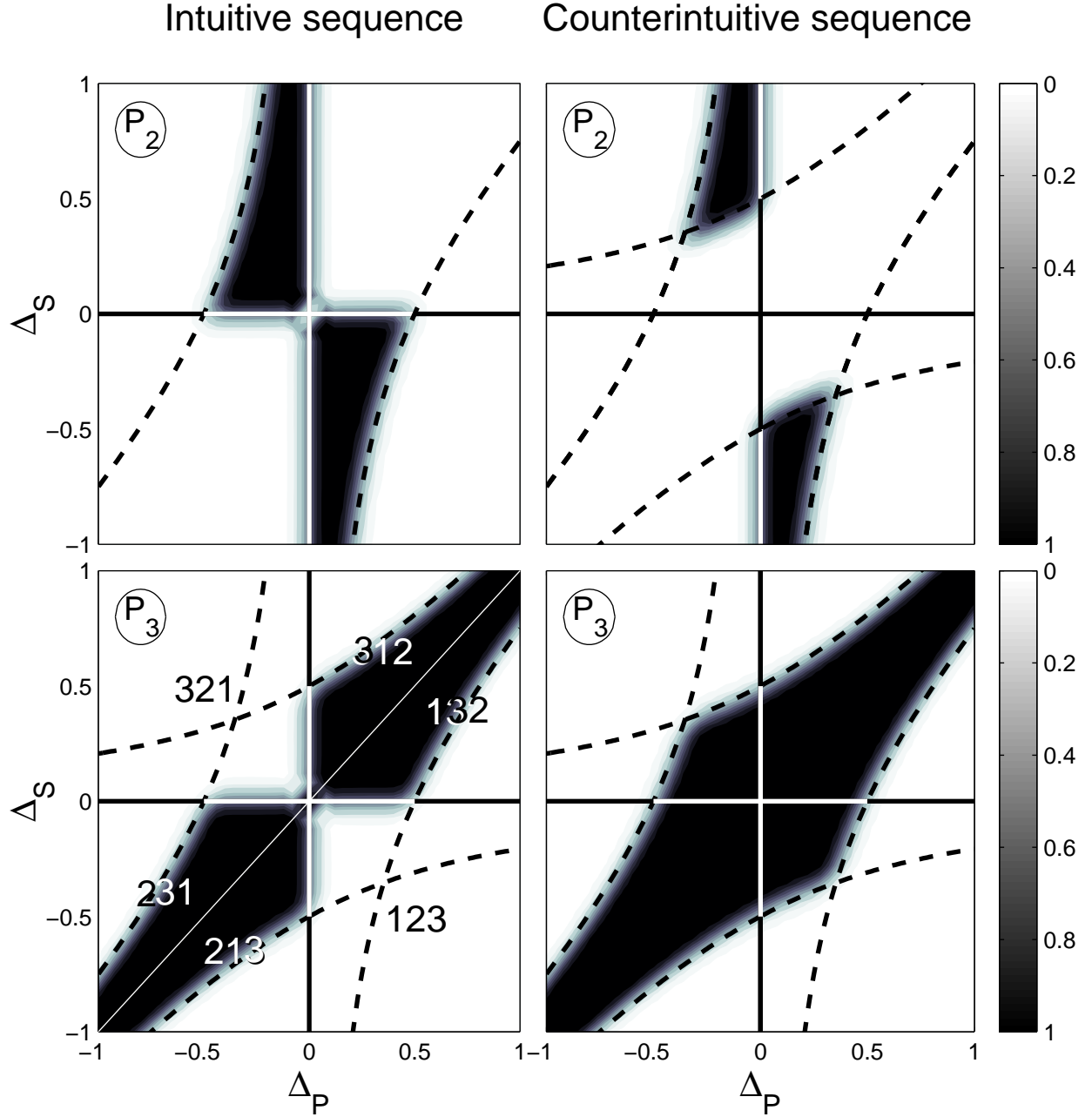


FIG. 7. Transfer efficiencies  $P_2$  to  $|2\rangle$  (upper row) and  $P_3$  to  $|3\rangle$  (lower row) at the end of the pulses for the intuitive (left column) and counterintuitive (right column) sequences of delayed sine-squared pulses with the same peak amplitude  $\Omega_{\max}$  and a large temporal area  $\Omega_{\max}\tau = 500$  ( $\tau$  is the pulse length and the delay is  $\tau/2$ ). The efficient population transfers are bounded by  $\Delta_P = 0$  and  $\Delta_S = 0$  (thick full lines) and the branches of hyperbolas (dashed lines). The areas bounded by the full lines are labelled by the cases 213, 132, 123, ... The three first ones correspond respectively to Figs 3, 4 and 5.

- [1] K. Bergmann, H. Theuer, and B. W. Shore, *Rev. Mod. Phys.* **70**, 1003 (1998).
- [2] M. M. T. Loy, *Phys. Rev. Lett.* **32**, 814 (1974).
- [3] R. G. Brewer and E. L. Hahn, *Phys. Rev. Lett.* **11**, 1641 (1975).
- [4] L. Allen and J. H. Eberly, *Optical Resonance and Two-Level Atoms* (Dover, New York, 1987).
- [5] H. P. Breuer and M. Holthaus *Phys. Lett. A* **140** 507 (1989).
- [6] S. Chelkowski, A. D. Bandrauk and P. B. Corkum, *Phys. Rev. Lett.* **65**, 2355 (1990).
- [7] S. Guérin, *Phys. Rev. A* **56**, 1458 (1997).
- [8] S. Chelkowski and A. D. Bandrauk, *J. Raman Spectroscopy* **28**, 459 (1997).
- [9] L. P. Yatsenko, B. W. Shore, T. Halfmann, K. Bergmann and A. Vardi, *Phys. Rev. A* **60**, R4237 (1999).
- [10] T. Ricketts, L. P. Yatsenko, S. Steuerwald, T. Halfmann, B. W. Shore, N. V. Vitanov and K. Bergmann, *J. Chem. Phys.* **113**, 534 (2000).
- [11] R. G. Unanyan, S. Guérin, and B. W. Shore, and K. Bergmann, *Eur. Phys. J. D* **8**, 443 (2000).
- [12] V. I. Romanenko, L. P. Yatsenko, *JETP* **90**, 407 (2000).
- [13] S. Guérin, L. P. Yatsenko and H. R. Jauslin, *Phys. Rev. A* (to be published).
- [14] H. R. Jauslin, S. Guérin and S. Thomas, *Physica A* **279**, 432 (2000).
- [15] B. W. Shore, *The Theory of Coherent Atomic Excitation* (Wiley, New York, 1990).
- [16] M. V. Danileiko, V. I. Romanenko, and L. P. Yatsenko, *Opt. Commun.* **109**, 462 (1994).
- [17] S. Guérin, L. P. Yatsenko, T. Halfmann, B. W. Shore, and K. Bergmann, *Phys. Rev. A* **58**, 4691 (1998).
- [18] D. Grischkowsky, M. M. T. Loy, P. F. Liao, *Phys. Rev. A* **12**, 2514 (1975).
- [19] M. L. Ter-Mikaelyan and R. G. Unanyan, *Laser Physics* **6**, 953 (1996).